



Trade Science Inc.

ISSN : 0974-7419

Volume 12 Issues 7

Analytical CHEMISTRY

An Indian Journal

Full Paper

ACAIJ, 12(7), 2013 [256-263]

Kinetic-spectrophotometric determination of tin species using feed- forward neural network and radial basis function networks in water and juices of canned fruits

Maryam Abbasi-Tarighat

Department of Chemistry, Faculty of Sciences, Persian Gulf University, Bushehr, 75169, (IRAN)

E-mail : matarighat@pgu.ac.ir; matarighat@gmail.com

ABSTRACT

Feed- forward neural network (FFNN) and radial basis function networks (RBFN) were used in the development of a kinetic-spectrophotometric method for the simultaneous determination of Sn(II) and Sn(IV). The two-way data matrices, based on changes of absorbance at the maximum wavelength of reaction products of Sn(II) and Sn(IV) with pyrocatechol-violet in acetate buffered solution (pH 4.0) were processed separately by the principal component-radial basis function-artificial neural network (exact fit and fewer neurons) and principal component feed-forward neural network (PC-FFNN). The network architecture (number of hidden, and output nodes), transfer functions, number of epochs, momentum and learning rate in FFNN model and spread value in radial basis function, were also optimized for getting satisfactory results with minimum errors. The proposed methods were successfully applied to determination of desirable metal ions in several synthetic samples. The results obtained by PC-FFNN and PC-RBF networks were compared to each other. The prediction performance of RBF network (exact-fit) was better than RBF (fewer neurons) network and PC-FFNN. The obtained satisfactory results indicate the applicability of ANNs approach for determination of desirable species. The proposed methods were successfully applied to the quantification of the Sn(IV) and Sn(II) in different water samples and canned products.

© 2012 Trade Science Inc. - INDIA

KEYWORDS

Simultaneous determination;
Tin;
Canned product.

INTRODUCTION

Spectrophotometric analysis of multicomponent mixtures shows that the quantification of compounds where there was no spectral difference had been a difficult problem. For solving this problem, during the last decades in many cases, kinetic-based methods continuously were applied^[1-3].

The chemometric methods including classical least squares (CLS), inverse least squares (ILS), principal component regression (PCR) and partial least squares (PLS) had been found increasing applications for multicomponent kinetic determination^[4-12]. These methods do not require prior knowledge of reaction order or reaction rate coefficient of the involved analytical systems. The predicted values of these methods will not in

good agreement with known values when nonlinearity presented in considered system.

An artificial neural network (ANN) is an interconnected group of artificial neurons that uses a mathematical model or computational model for information processing^[13-15]. The multi-layer feed-forward neural networks (FFNNs) with the error back-propagation learning rule is the technique most frequently used. Radial basis function (RBF) networks on the other hand, offer interesting alternatives to FFNNs in the sense that they allow local training^[16-17]. Radial basis function networks possess a best property of best approximation and may require more neurons than feed-forward back propagation networks^[18-22].

A different approach to carry out multicomponent kinetic determinations was proposed based on artificial neural network (ANN) models^[23,24]. Also for resolve three dimensional data (combination of kinetics and spectroscopy data) the multidimensional partial least square (NPLS) and the parallel factor (PARAFAC) analysis was presented^[25,26]. However three way data matrix can be developed based on the so called second order advantage, i.e. robust estimation of the analytes concentration in mixtures that contain unknown interferences. But the number of studies using experimental data is still very limited. For example PARAFAC has a basic trilinear model which is compatible with analytical data structures involving spectrophotometric measurements.

Tin can enter your body when you eat contaminated food or drink contaminated water, when you touch or eat soil that has tin in it, or when you breathe tin-containing fumes or dusts. When you eat tin in your food, very little leaves the gastrointestinal tract and gets into your bloodstream. The presence of tin in fresh food of both vegetable and animal origin is highly dependent on the concentration of tin in the soil of the area in which the food is produced. There is no evidence that tin is an essential element for humans. Exposure to Sn and its compounds can produce several effects such as neurological, hematological and immunological. Inhalation of iSn can induce to pneumoconiosis and ingestion may lead to gastrointestinal effects. Despite the dangers they are applied in a great number of industries, such as the paint industry and the plastic industry, and in agriculture through pesticides. Tin metal is used as a protective

coating in food, beverage and aerosol cans. Canning may result in dissolution of the tin lining of the can, particularly if the products are acidic.

Determination of tin species, mainly their organometallic derivatives, is among the most required analysis in environmental studies, not only due to their toxicity, but also because they are good indicators of anthropogenic pollution sources^[27,28]. In the literature, several methods for determination of tin were proposed^[28-32]. To the best of our knowledge less attention has been paid to simultaneous determination of Sn(IV) and Sn(II). Recently, Afkhami et al., developed mean centering of ratio kinetic profiles and partial least squares (PLS) methods for the simultaneous analysis of binary mixtures of Sn(II) and Sn(IV)^[33].

De Azevedo et al., developed a procedure for the determination of tin in whole blood and urine by GF AAS with a minimum sample pre-treatment, using Pd/Mg as chemical modifier^[34].

ANNs are powerful chemometric methods because they do not need any model structure specification and can process multivariate problems of nonlinear systems. With proper training, ANNs can accurately model the presence of synergistic effects and avoid the potential loss of kinetic data for mixtures resulting from too short induction periods, outliers, and small differences in the rate constants, and so on. The purpose of this study is to compare performances of the principal component-radial basis function networks and principal component-feed forward neural networks for multi-component determination based on difference in kinetic rates of Sn(II) and Sn(IV) by PCV. We created *exact fit* – PC-RBF, *fewer neuron*-PC-RBF and PC-FFNN that they are often used for determination. To our knowledge this is first report on applicability of RBF for kinetic- spectrophotometric determination of Sn(II) and Sn(IV). The variations of absorbance of the complexes were monitored at maximum wavelength of 550 nm. The part of data from 0 to 10 min was applied for analysis. Simultaneous determination can be performed without carefully controlling experimental conditions and also with handling non-linearities due to kinetic parameters. By using the two way data (absorbance measurement at a single wavelength by changing the concentration of reactants) the metal ions were estimated. The obtained results of PC-RBF (*exact fit* and *fewer neurons*) and

Full Paper

PC-FFNNs were compared with each others and those obtained from previous work^[33]. The methods were validated by determining Sn(II) and Sn(IV) in synthetic mixtures, tap water, river water and canned products.

EXPERIMENTAL

Reagents

All solutions were prepared with analytical grade reagents. Stock solutions of Sn(II) and Sn(IV) ($100 \mu\text{g mL}^{-1}$) were prepared by dissolving appropriate amounts of $\text{SnCl}_2 \cdot 2\text{H}_2\text{O}$ (Merck) and $\text{SnCl}_4 \cdot 5\text{H}_2\text{O}$ (Fluka), respectively, in 0.2 mol L^{-1} HCl. A $1.0 \times 10^{-3} \text{ mol L}^{-1}$, Pyrocatechol-violet (PCV) (Merck) solution was prepared daily by dissolving appropriate amount of this indicator in doubly distilled water. Acetic acid-acetate (1.0 mol L^{-1}) buffer solution of pH 4.0 was prepared from acetic acid and sodium acetate (Merck).

Apparatus

A Perkin-Elmer Lambda 45 UV-vis spectrometer was used for recording and storage of UV-vis absorbance spectra using 1 cm quartz cells and slit width of 0.5 nm. The ANN algorithm (nntool) was run in MATLAB (Math Work, version 7.1).

Procedure

Two ml buffer solution and 1.68 mL of PCV solution and desirable concentration of metal ions were added to a 5 ml volumetric flask and made up to the mark with water. A portion of the solution was transferred into a quartz cell to record the absorption kinetic profile of the solution at 550 nm in the time range 0–10 min with 1 s intervals.

(a) Theory of RBF networks

A radial basis function (RBF) is a real-valued function. The structure of radial basis function networks (RBFN) is comprised three units of input, hidden and output. The input units serve only to distribute input to hidden unit. Each neuron of the hidden unit represents a basis functions, with equal dimensions to the input data. RB networks generally use a Gaussian function to account for the non-linearity of the hidden unit processing elements. The Gaussian function responds only to a small region of the input space where the Gaussian is centered. The successful implementation of these networks

is to find suitable centers for such a Gaussian functions, which is characterized by two parameters, i.e. Center (c_j), and peak width (δ_j). The RBF are typically used to build up the output of the form

$$\text{out}_j = \phi(\|x_j - c_j\|) = \exp\left(-\frac{\|x_j - c_j\|^2}{\delta_j^2}\right) \quad (1)$$

where $\|x_i - c_j\|$ is the calculated Euclidean distance between x_i and c_j , and δ_j determines the portion of the input space where the j th RBF will have a non-significant zero response. The input value to each output node is the weighted sum of all the outputs of the hidden nodes. Finally, the response of each output node is calculated by a linear function of its input (including the bias w_{k0}), what is, the output of hidden layer (out_k). The relation between the value out_k and the input variable x_i can be represented by:

$$\text{out}_k = w_{k0} + \sum_j w_{kj} \phi(\|x_i - c_j\|) \quad (2)$$

The weights w_{kj} are adjusted to minimize the mean square error of the net output.

(b) Optimization of experimental conditions

The optimum conditions for simultaneous determination of Sn(II) and Sn(IV) were chosen as follows: pH is 4.0 and an excess amount of PCV ($3.2 \times 10^{-4} \text{ mol L}^{-1}$) was applied to obtain a pseudo-first order reaction with respect to each cation.

RESULTS AND DISCUSSION

Kinetic-spectral nature of the metal– pyrocatechol violet

Sn(IV) and Sn(II) can react with PCV to form a colored complex. They show maximum absorbance at 550 nm. Figure 1 shows the spectrum of individual of component at presence of PCV in 10 min. Simultaneous determination of desirable metal ions due to lack of spectral discrimination were impossible (Figure 1).

The reaction rate of Sn(IV) and Sn(II) were different and for Sn(IV) was faster. This difference gives the possibility for resolving their mixtures (Figure 2) in simultaneous determination of two metal ions. Absor-

bance monitoring at single wavelength has a great advantage in determination of Sn(II) and Sn(IV) when diode array spectrophotometer not be available in each laboratory. Principal component analysis was performed on the created two way data which obtained by measuring the absorbance at a single wavelength after changing the concentration of Sn(II) and Sn(IV). Optimal numbers of principal components (PCs) were used as inputs for calibration of artificial neural networks.

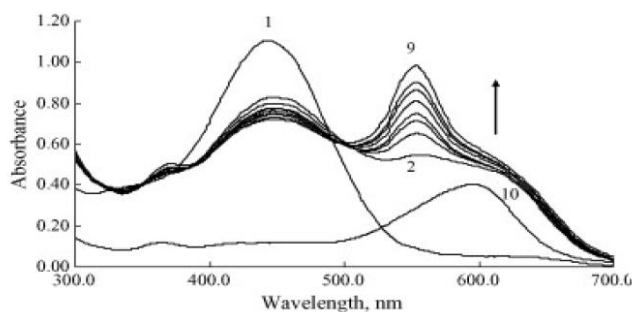


Figure 1 : Absorption spectra of Sn(II) and Sn(IV) by PCV at $3.2 \times 10^{-4} \text{ mol L}^{-1}$ PCV and 0.60 mg L^{-1} Sn(II) and Sn(IV) at pH 4.0.

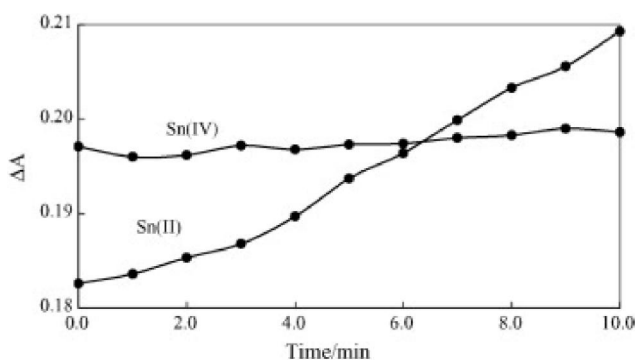


Figure 2 : The kinetic profiles of complexation reactions of Sn(II) and Sn(IV) with PCV at 550 nm, conditions: PCV concentration $3.2 \times 10^{-4} \text{ mol L}^{-1}$, the concentration of Sn(II) and Sn(IV) was 0.60 mg L^{-1} at pH 4.0.

Network optimization

(a) Calibration of PC-FFN networks

The kinetic data obtained from experiments were processed by FFNN, which was trained with back-propagation of errors learning algorithm. The aim of calibration is to produce a model that relates the kinetic spectral data of calibration mixtures to the concentration data. If we suppose calibration set with m samples containing n analytes with the absorbance obtained at t times, then in the learning procedure for the first analyte, the $m \times t$ data matrix is fed into the network with output vector $n \times r$ concentration set of desired analyte).

The response of network with one hidden layer and one output neuron, out_k , to the input vector x_i , is the calculated concentration that can be written as eq. 1:

$$\text{out}_k = g \left(\sum_{j=1}^h w_{jk} f \left(\sum_{i=1}^k w_{ij} x_i + b \right) + b' \right) \quad (3)$$

Where f is the transfer function applied for hidden layer, g the transfer function applied for hidden layer, b and b' are the biases of the model, w_{ij} the weight value from the input neurons to the hidden neurons, w_{jk} the weight from hidden neurons to the output neuron and h the neuron number in the hidden layer. The network output, out_k , is compared with desired output and the error term is calculated. During the training process, the weights are iteratively calculated in order to minimize the sum of squared difference between the known concentrations and the calculated concentrations. The training was stopped manually when the root mean square error of the test set remained constant after successive iteration. The neural network models were tested on an external prediction set (validation set) that consisted of samples belonging to neither the calibration set nor test set.

The chose architecture for comparison was that which produced the minimum relative standard error of prediction (RSE %) as eq.2:

$$\% \text{RSE} = \sqrt{\frac{\sum_{i=1}^{np} (C - C_p)^2}{\sum_{i=1}^{np} C}} \times 100 \quad (4)$$

Where np is the number of the samples used in validation set, C real value and C_p the predicted value. In these work, the whole data set (34 synthetic sample mixtures) was prepared randomly from concentrations of both analytes to cover the measuring range. The synthetic sample mixtures were randomly distributed into three sets, i.e. calibration set, test set and validation set with sizes 20, 13 and 6 respectively. The former was used to train the network and second for testing and the third was used to validate the learned network.

The numbers of input nodes were selected as an optimal number of principal components which obtained by applying principal component analysis on two way kinetic data. To optimization of network architecture, number of hidden layers was varied from one to five

Full Paper

(Figure 3). As the Figure 3 shows the RSE% was minimum at one layer. The effected number of hidden neurons was determined by training PC-FFNN with different number of neurons. As observed in Figure 4 a minimum in RSE% occurred when proper neurons four and three were used in the hidden layer for Sn(IV) and Sn(II) respectively. The basic transfer function used here consisted of a Logistic function, which passes the value through a non-linear function for hidden layer and pureline for output layer.

The output layer for Sn(IV) and Sn(II) was one layer. Training the network was performed with several learning rates which changed from 0.01 to 0.1. During the learning procedure of the network with the calibration set, the test set was subsequently tested with the learned network. The results for optimized parameters for construction of the network are represented in TABLE 1.

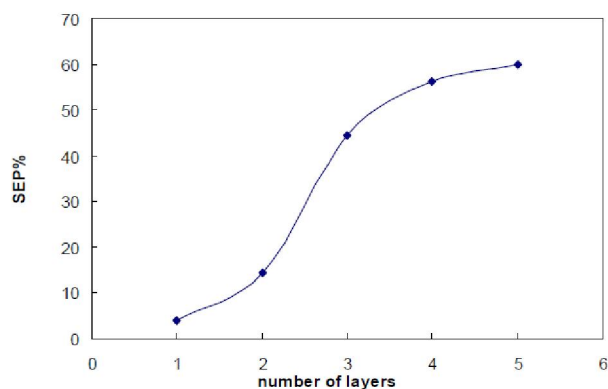


Figure 3 : Plots of RSE% as a function of the number of layers for selection of hidden layer for Sn(II) (\blacktriangle) and Sn(IV) (\blacksquare) in determination by FFNN.

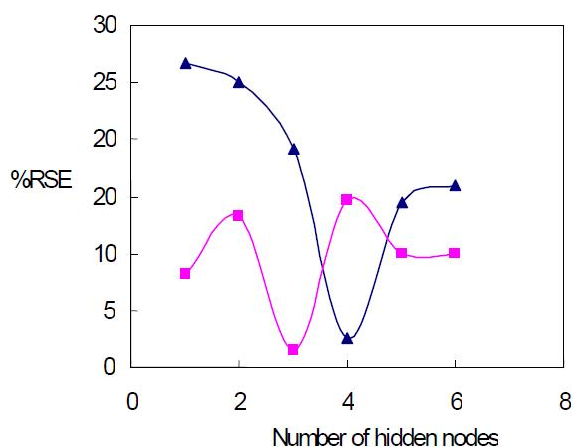


Figure 4 : Plots of RSE% as a function of the number of neurons in hidden layer for Sn(IV) (\blacktriangle) and Sn(II) (\blacksquare) in determination by FFNN.

TABLE 1 : Optimized parameters used in PC-FFNNs at simultaneous determination of Sn(IV) and Sn(II) by PCV.

Parameter	Compound	
	Sn(IV)	Sn(II)
Input nodes	3	3
Hidden nodes	4	3
Output nodes	1	1
Learning rate	0.1	0.1
Momentum	0.01	0.01
Number of iteration	850	1000
Hidden layer transfer function	Logsig	Logsig
Output layer transfer function	Purelin	Purelin

By optimized parameter in TABLE 1 the network architectures for two ion metals was created and concentration of each ion was predicted. TABLE 2 shows the results obtained for prediction samples by PC-FFNN. The reasonable relative errors for each analyte in both sets calculated by eq.2, for each analyte in this set indicate the applicability of the proposed method.

TABLE 2 : Prediction results obtained Sn(IV) and Sn(II) in simultaneous determination with PC-FFNN.

Actual/ $\mu\text{g mL}^{-1}$		Found/ $\mu\text{g mL}^{-1}$	
Sn(IV)	Sn(II)	Sn(IV)	Sn(II)
0.50	0.00	0.50	0.51
0.60	1.00	0.61	0.00
1.00	0.80	0.98	0.99
0.30	0.60	0.32	0.78
0.50	0.60	0.51	0.61
0.90	0.30	0.90	0.62
0.50	0.90	0.49	0.32
0.50	0.60	0.50	0.89
0.60	0.80	0.61	0.58
0.60	0.00	0.61	0.78
0.60	1.00	0.60	0.00
0.00	0.00	0.00	1.00
1.60		1.57	0.00
R.S.E%		1.79	1.96
Mean R.S.E%		1.87	

(b) Calibration of RBF networks

In RBF networks, two sets of parameters (the centers and the widths) in the hidden layer and a set of weights in the output layer are adjusted. Therefore, the adjustment of the output layer is simple and RBFN has a guaranteed learning procedure for converge. How-

ever, in back-propagation FFNN, the parameters of transfer functions both in hidden and output layers should be adjusted by using the Sigmoid transfer functions and generally it is time consuming. For the determination of tin species, the *exact fit* type of radial basis from MATLAB 7.1 was selected. In this procedure the numbers of hidden nodes are equal to the number of nodes in the input layer. So, the adjustable parameters were the number of input variable and spread. Input variables for this part were first four principal components. The latter parameter was in relation with the spread of radial basis functions in the network. RSE% for the prediction of both of Sn(II) and Sn(IV) at the spread values of 1-50 were investigated (Figure 5).

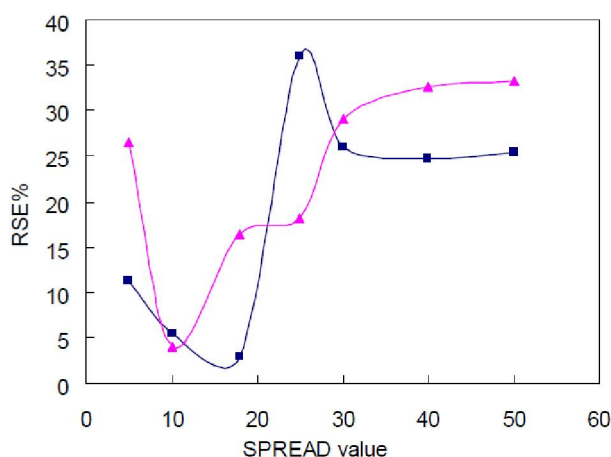


Figure 5 : Plots of RSE% as a function of spread for Sn(IV) (▲) and Sn(II) (■) in determination by RBFN.

The obtained results from repetition of training procedure of PC-RBF, for each condition were the same. It was due to high reproducibility of modeling that is a main advantage for the RBFN. In this way, 3 times repetition of training in each of experimental condition was performed (TABLE 3).

Also same procedure was applied for the simultaneous determination of tin species; by *fewer neurons* -RBF from MATLAB 7. In this case the number of inputs was same as *exact fit* type but optimal amount of SPREAD value was 25 for both of metal ions. By the optimal parameters the concentration of Sn(II) and Sn(IV) was predicted. The result of prediction set which obtained by *fewer neurons* -RBF are presented in TABLE 3.

The ANNs have been trained on the same datasets. To evaluate the performance of neural networks, the RSE% of its results compared with the RSE% of the

mean centering (MC) and PLS as well as previous one^[31]. The RSE% for Sn(II) and Sn(IV) were 3.76 and 3.80%, respectively by MC and Sn(II) and Sn(IV) were 4.5 and 1.80% respectively by PLS. These reveal the superiority of neural networks over the other methods. The superiority of the neural networks over the MC and PLS is partly due to the fact that in neural networks the interactions between different parameters used as considered. By considering the results of TABLE 2 and TABLE 3 it was cleared that the calculated values by fPC-RBF (*exact fit* and fewer neurons) are better than that obtained and PC-FFNN. However the performance of two types of RBF networks (*exact fit* and fewer neurons) had not much difference but *exact fit* -RBF performed better than *fewer neurons*-RBF in predicting of Sn(IV) and Sn(II) concentrations. It was due to local training ability of RBF and interpretation of final model in terms of logical rules. RBF networks are able to detect new local generalization. This one is obtained by the Gaussians basis functions that are maximal to the core, and decrease in a monotonous way with the distance. On the other hand, Due to the localized nature of RBFN, the network can be trained extremely quickly and facilitates nonlinear calculation. Therefore, the precision and accuracy of RBFNs results are better than FFNN results.

TABLE 3 : Prediction results obtained in simultaneous determination of Sn (IV) and Sn(II) by (a)*exact fit*-PC-RBF and (b)*fewer neurons*-PC-RBF.

Actual / $\mu\text{g mL}^{-1}$		^a Found / $\mu\text{g mL}^{-1}$		^b Found / $\mu\text{g mL}^{-1}$	
Sn(IV)	Sn(II)	Sn(IV)	Sn(II)	Sn(IV)	Sn(II)
0.50	0.50	0.50	0.51	0.51	0.51
0.60	0.00	0.60	0.00	0.60	0.00
1.00	1.00	0.98	1.00	1.02	1.01
0.30	0.80	0.30	0.81	0.29	0.82
0.50	0.60	0.51	0.60	0.50	0.61
0.90	0.60	0.90	0.61	0.90	0.60
0.50	0.30	0.49	0.31	0.50	0.30
0.50	0.90	0.52	0.91	0.51	0.91
0.60	0.60	0.61	0.60	0.60	0.61
0.60	0.80	0.62	0.81	0.60	0.80
0.60	0.00	0.60	0.00	0.61	0.00
0.00	1.00	0.00	1.00	0.00	0.97
1.60	0.00	1.59	0.00	1.58	0.00
R.S.E%		1.52	1.04	1.31	1.84
Mean R.S.E		1.28		1.57	

Full Paper

TABLE 4 : Simultaneous determination of Sn(IV) and Sn(II) in different water samples by the proposed methods.

Method	Actual/ $\mu\text{g mL}^{-1}$		Found / $\mu\text{g mL}^{-1}$	
	Sn(II)	Sn(IV)	Sn(II)	Sn(IV)
FFNNs	1.00 ^a	1.20 ^a	1.18±0.00	1.33±0.00
	0.80 ^b	0.70 ^b	0.81±0.01	0.68±0.11
FFNNs	1.00 ^a	1.20 ^a	1.10±0.00	1.20±0.00
	0.80 ^b	0.70 ^b	0.08±0.0	0.69±0.11

spiked in tap water and (b) spiked in river water

Application of the methods

To test the accuracy of the method, known amounts of Sn(II) and Sn(IV) were spiked into several tap water and river water samples (TABLE 4). The appropriate amounts of PCV and solution of buffer were added afterward. The proposed methods were applied to the determination of the analytes, and satisfactory results were obtained (TABLE 4).

The proposed methods were successfully applied to the simultaneous determination of metal ions in canned orange and pineapple juice samples (TABLE 5).

For digestion of the sample, five milliliters of orange juice or pineapple juice was transferred into a 250 mL Erlenmeyer flask and 10 mL of concentrated sulfuric acid was added. The solution was diluted to about 75 mL by distilled water. Then, it was cooled, filtered and washed with water and the filtrate was collected in a 100 mL calibrated flask and diluted to the volume with water. The 2.0 mL of the solution and optimal amount of PCV and buffer solution were transferred in volumetric flask and diluted to the mark. The absorbance of this solution was recorded. The concentration of Sn(II) and Sn(IV) was determined by the PC-FFNNs and PC-RBF networks. Total concentration of tin in the samples was also determined by flame atomic absorption spectrometry (FAAS). The total amount of Sn(II) and Sn(IV) obtained by FAAS were 57.60 $\mu\text{g mL}^{-1}$, 61.84 $\mu\text{g mL}^{-1}$ and 70.50 $\mu\text{g mL}^{-1}$ for orange juice 1, orange juice 2 and pineapple juice samples, respectively.

The total amounts of Sn(II) and Sn(IV) which obtained by the proposed methods were in good agreement with those obtained by FAAS. The results are shown in TABLE 5. The predicted concentrations of Sn(II) and Sn(IV) in different fruit juice samples show that the predicted results are in good consistent with

the standard values. Moreover the calculated results proved that the proposed neural networks approach based on the PCA input selection was suitable for the simultaneous determination of Sn(II) and Sn(IV) in different samples.

TABLE 5 : Concentration and recoveries of Sn(IV) and Sn(II) in fruit juices samples by the proposed and standard methods.

Sample	Added/ $\mu\text{g mL}^{-1}$		Found/ $\mu\text{g mL}^{-1}$					
			PC-FFNN		Exact fit-P RBF		Fewer neuron PC-RBF	
	Sn(IV)	Sn(II)	Sn(IV)	Sn(II)	Sn(IV)	Sn(II)	Sn(IV)	Sn(II)
Orange juice (1)	-	-	31.24	28.10	29.88	26.60	30.20	28.20
	8	6	40.26	32.88	38.32	32.95	39.42	33.90
Recovery%	-	-	102.5	96.42	101.14	101.0	103.1	99.12
Orange juice (2)	-	-	34.52	29.25	33.54	30.54	33.52	30.45
	8	6	44.70	34.65	42.32	36.95	43.27	35.18
Recovery%	-	-	105.1	98.3	101.8	101.1	104.2	96.51
Pineapple juice	-	-	40.35	28.62	37.50	31.72	40.4	27.72
	8	6	49.87	33.32	46.94	38.67	47.28	33.24
Recovery%	-	-	103.1	96.24	103.1	102.5	97.69	98.58

CONCLUSION

This study has shown that the PC-RBF (exact fit and fewer neurons) and PC-FFNN are the most effective for simultaneous kinetic determination of binary mixtures. Because lack spectral discrimination between the product of reaction of Sn(II) and Sn(IV) by PCV were presented, differences in their rates of reaction afford their quantitation with an ANN models. Hence, not necessary to use all of the analytical information acquired such as absorbance, times, and all wavelengths; rather, one can use only data recorded at the maximum absorbance of product. Determination of them was performed by PC-FFNNs and PC-RBFN. The proposed methods are very selective, sensitive and do not need any separation steps in simultaneous determination of both metal ions. These methods are offering acceptable methods for the determination of Sn(II) and Sn(IV) in routine analysis. At the RBF training, the obtained results from repetition of training procedure, are close to each other and not large different. It was due to high reproducibility of the RBF modeling that it can be a main advantage for the RBFN. Satisfactory results created by RBFN shows, the modeling have a powerful poten-

tial for the considered system without knowledge of the kinetic rate constant and reaction order. High reproducibility of training procedure and considerably lower training period (due to less obtainable parameters) in the RBFN are among the main advantage of these networks compared to FFNNs. The RBF network especially *exact fit-RBF* can be effective calibration method for the kinetic determination of highly spectral overlapping systems.

REFERENCES

- [1] H.A.Mottola; Kinetic aspects of analytical chemistry, John Wiley, New York, (1988).
- [2] D.Perez-Bendito, M.Silva Kinetic; Methods in analytical chemistry, Ellis Horwood, Chichester, UK, (1988).
- [3] D.Perez-Bendito; Analyst, **115**, 689 (1990).
- [4] A.K.Pettersson, B.Karlberg; Anal.Chim.Acta, **354**, 241 (1997).
- [5] Y.L.Xie, J.J.Baeza-Baeza, G.Ramis-Ramos; Chemom.Intell.Lab.Syst., **27**, 211 (1995).
- [6] G.Lopez-Cueto, J.F.Rodriguez-Medina, C.Ubide; Analyst, **122**, 519 (1997).
- [7] W.Wu, R.Manne; Chemom.Intell.Lab.Syst., (51), 145 (2000).
- [8] A.Afkhami, M.Bahram; Talanta, **68**, 1148 (2006).
- [9] D.M.Haaland, R.G.Easterling; Appl.Spectrosc., **34**, 539 (1980).
- [10] C.W.Brown, P.F.Lynch, R.J.Obremski, D.S.Lavery; Anal.Chem., **54**, 1472 (1982).
- [11] H.J.Kisner, C.W.Brown, G.J.Kavarnos; Multiple analytical frequencies and standards for the least-squares spectrometric analysis of serum lipids. Anal.Chem., **55**, 1703 (1983).
- [12] T.Jolliffe; Principle component analysis, Springer, New York, (1986).
- [13] L.Zupan, J.Gasteiger; Anal.Chim.Acta, **248**, 1 (1991).
- [14] F.Despaigne, D.L.Massart; Analyst, **123**, 20 (1998).
- [15] D.A.Cirovic; Trends Anal.Chem., **16**, 148 (1997).
- [16] E.P.P.A.Derks, M.S.Sanchez Pastor, L.M.C.Buydens; Chemom.Intell.Lab.Syst., **2**, 49 (1995).
- [17] B.Walczak, D.L.Massart; Anal.Chim.Acta, **331**, 177 (1996).
- [18] S.Chen, C.F.N.Cowan, P.M.Grant; IEEE Transactions on Neural Networks, **2**, 302 (1991).
- [19] Y.L.Loukas; Anal.Chim.Acta, **417**, 221 (2000).
- [20] Z.Zhang, D.Wang, P.B.Harrington, K.J.Voorhees; J.Rees.Chen.Talanta, **17**, 527 (2004).
- [21] Y.Dou, H.Mi, L.Zhao, Y.Ren; Spectrochim Acta Part A, **65**, 79 (2006).
- [22] N.Qu, X.Li, Y.Dou, H.Mi, Y.G.Ren; European Journal of Pharmaceutical Sciences, **31**, 206 (2007).
- [23] S.Ventura, M.Silva, D.Perez-Bendito, C.Hervas; Anal.Chem., **67**, 4458 (1995).
- [24] M.Blanco, J.Coello, H.Iturriaga, S.Maspoch, M.Redon; Anal.Chem., **67**, 4477 (1995).
- [25] R.Bro; Chemom.Intell.Lab.Syst., **38**, 149 (1997).
- [26] Y.Ni, C.Huang, S.Kokot; Anal.Chim.Acta, (599), 209 (2007).
- [27] M.Hoch; Appl.Geochem., **16**, 719 (2001).
- [28] R.P.Mason, W.F.Fitzgerald, F.M.M.Morel; Cosmochim.Acta, **58**, 3191 (1994).
- [29] L.Clinio, T.Giancarlo; Microchem.J., **78**, 175 (2004).
- [30] Y.Li, H.Long, F.Zhou; Anal.Chim.Acta, **554**, 86 (2005).
- [31] S.Rubio, A.Gomez-Hens, M.Valcarcel; Analyst, **110**, 43 (1985).
- [32] J.L.Manzoori, M.Amjadi, D.Abolhasani; J.Hazard.Mater.B, **137**, 1631 (2006).
- [33] T.Madrakian, A.Afkhami, R.Moein, M.Bahram; Talanta, **72**, 1847 (2007).
- [34] S.V.De Azevedo, F.R.Moreira, R.C.Campos; Clinical biochemistry, <http://dx.doi.org/10.1016/j.clinbiochem.2012.09.020>